Impact of four-phonon scattering on thermal transport in carbon nanotubes

Ankit Jain[*]

Mechanical Engineering Department, IIT Bombay 400076, India

The thermal transport properties of single-wall carbon nanotubes (SWCNTs) are reinvestigated using the iterative solution of the Boltzmann transport equation by including four-phonon scattering. Using only three-phonon scattering, the flexural and twisted phonon modes are found to remain nonscattered via Umklapp processes. However, with four-phonon scattering, while longitudinal modes remain unaffected, the transverse modes undergo Umklapp scattering. The predicted thermal conductivity of SWCNTs using both three- and four-phonon scatterings is 4000 W/m-K at 300 K, and stays highest amongst all known materials.

I. INTRODUCTION

The understanding of thermal transport physics of carbon nanotubes has remained an open research problem to date [1–10]. Experimentally, on the one hand, the thermal transport in single-wall carbon nanotubes (SWCNTs) is measured to be nondiffusive with divergence of thermal conductivity (κ) for tube lengths of up to 1 mm [6,8], as suggested by the Fermi, Pasta, Ulam (FPU), and Tsingou model [11], on the other hand, the κ is recently reported to converge for tube lengths of only 10 μm [12], thus, highlighting challenges in the experimental measurements and interpretation of thermal transport results for SWCNTs [13].

Earlier theoretical studies, based on phonon scattering selection rules, suggested nonscattering of long wavelength flexural acoustic and twisted/rotational acoustic phonon modes (collectively referred to as transverse modes, hereafter) via the Umklapp three-phonon processes [7,14]. This is indeed confirmed numerically from mode-dependent phonon properties obtained by employing the iterative solution of the Boltzmann transport equation (BTE) where κ is found to diverge in the absence of phonon-boundary scattering [7]. These theoretical predictions and numerical mode-dependent phonon properties are, however, obtained by considering only three-phonon processes, and it is not clear if the long wavelength transverse phonon remains unscattered when higher-order four-phonon processes are accounted for [7,9]. Other computational approaches based on molecular dynamics simulations can naturally include phonon anharmonicity to the highest order. However, these simulations remained inconclusive for SWCNTs with equilibrium molecular dynamics suggesting converged κ [5,15], and the direct molecular dynamics suggesting length dependence of κ for up to at least 10 μm [4,16].

With recent advances in computational resources, it is now becoming possible to include higher-order four-phonon processes in the prediction of phonon transport properties via the BTE-based approach [17–21]. However, due to several

orders of magnitude higher computational cost of four-phonon processes compared to the three-phonon counterpart [17], the application of four-phonon processes is currently limited to simple material systems with fewer than 8–10 atoms in the unitcell [17–22]. For the particular case of carbon-based reduced dimensionality systems, such as graphene and CNTs, this is even more challenging as the BTE is required to be solved iteratively for the correct description of Normal and Umklapp phonon processes [7], and thus requiring evaluation of four-phonon scattering rates at each iteration step.

In this work, the thermal transport properties of (10,0) SWCNTs consisting of a 40 atom unitcell are evaluated by considering both three- and four-phonon processes by employing the iterative solution of the BTE.

II. METHODOLOGY

The thermal transport in metallic/semimetallic SWCNTs is predominantly due to atomic vibrations, i.e., phonons [23]. The κ of phonon is obtainable from BTE along with the Fourier law as [21,24]

$$\kappa = \sum_i c_{ph,i} v^2 \tau_i, \tag{1}$$

where the summation is, over all the phonon modes in the Brillouin zone, enumerated by $i \equiv (q, \nu)$, where q and ν are phonon wave vector and mode index, and $c_{ph,i}$, v, and τ_i represent phonon specific heat, group velocity, and transport lifetime, respectively. The phonon transport lifetimes are obtained from the iterative solution of the BTE by considering phonon-phonon scattering via three- and four-phonon scattering processes, and phonon-boundary scattering corresponding to a characteristic length scale, L, as $\tau_{bdry} = L/2|v|$. Instead of phonon transport lifetimes, if phonon relaxation lifetimes are employed in Eq. (1), then it corresponds to the well-known relaxation time approximation (RTA) of the BTE. Further details regarding the calculation of phonon heat capacity, group velocity, and relaxation/transport lifetimes are presented in Refs. [18,21]. The phonon modes are classified as longitudinal when participating atoms are majorly displaced along the length of the tube, i.e., $|\mathbf{e_i} \cdot \hat{\mathbf{n}}| > 0.5$, where $\mathbf{e_i}$ represents the

*a_jain@iitb.ac.in

eigenvector of the concerned phonon mode and $\hat{\mathbf{n}}$ is a unit vector along the length of the tube. The modes which are not longitudinal are classified as transverse modes.

III. COMPUTATIONAL DETAILS

The computation of phonon thermal conductivity via Eq. (1) requires harmonic, cubic, and quartic interatomic force constants [21]. The harmonic force constants are obtained using density functional perturbation theory (DFPT) [25], as implemented in the planewaves-based quantum simulation package QUANTUM ESPRESSO [26] with PBEsol pseudopotentials [27], with converged electronic wave vector grid and plane wave energy cutoff of size 10 and 80 Ry, respectively. The harmonic force constants are initially obtained on a phonon wave vector grid of size 10 (with 40 atoms unitcell) and are later interpolated to a finer grid of size $N_q = 100$ for phonon-phonon scattering rate calculations (120 for four-phonon processes). The anharmonic force constants are obtained by least square Taylor series fitting of force-displacement data obtained from randomly displacing atoms by 0.05 or 0.10 Å from their equilibrium positions. 600 such structures, each with 200 atoms in the supercell (five repetitions of unitcell along the tube length), are considered for the force-displacement dataset which results in a highly over-determined system with 120 times more equations than the number of unknowns. The cubic and quartic interaction cutoffs are set at the fourth and first neighbor shell. The change in κ obtained using the relaxation time approximation (RTA) solution of BTE, and using only three-phonon scattering, is less than 6% in changing the cubic interaction cutoff from fourth to third neighbor shell at 300 K. The harmonic, cubic, and quartic interatomic force constants are provided in the Supplemental Material (SM) along with comparison of randomly displaced Taylor-series fitting and finite-difference based force constants (Fig. S1) [28].

IV. RESULTS

The structure of considered SWCNT and phonon dispersion are presented in Fig. 1. The considered SWCNT is an achiral zigzag (10,0) with 40 atoms in the unitcell (highlighted in cyan in Fig. 1) and 7.89 Å diameter. While the phonon dispersion of SWCNTs is discussed in detail in many studies (from theoretical and analytical/empirical forcefields) [7,9], it is worth emphasizing that in the long wavelength limit, the flexural acoustic phonon modes (doubly degenerate) have quadratic phonon dispersion. In contrast, the twisted/rotational and longitudinal modes have linear dispersions. The phonon velocities for twisted and longitudinal modes from DFPT obtained here are 13.2 and 21.1 km/s compared to 13.6 and 21.4 reported by Bruns *et al.* [29] using the empirical Tersoff forcefield.

Considering only three-phonon scattering and empirical Tersoff potential, Lindsay *et al.* [7] found that acoustic phonons fail to satisfy scattering conservation rules and cannot undergo Umklapp scattering with other acoustic phonons. They found that using the RTA solution of the BTE, which wrongly treats population redistributing Normal processes as resistive, the κ of SWCNT converges with length, but when
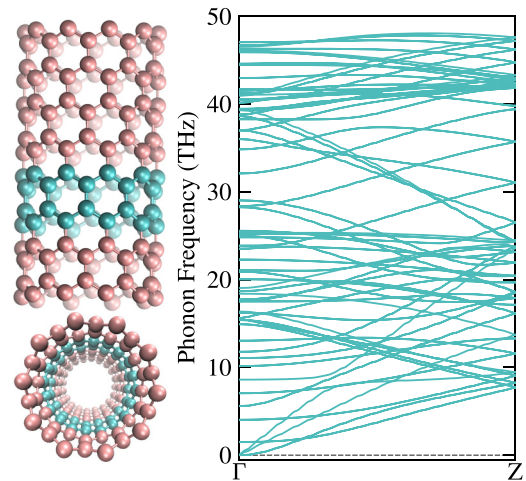

FIG. 1. The phonon dispersion of considered SWCNT. The structure of considered SWCNT is shown in the left and has 40 atoms in the unitcell (highlighted with a cyan color).

the iterative solution of the BTE is employed to correctly describe Normal and Umklapp processes, κ increases more than twofold. Similar findings are recently also reported by Bruns *et al.* [9]. In this work, using only three-phonon scattering,
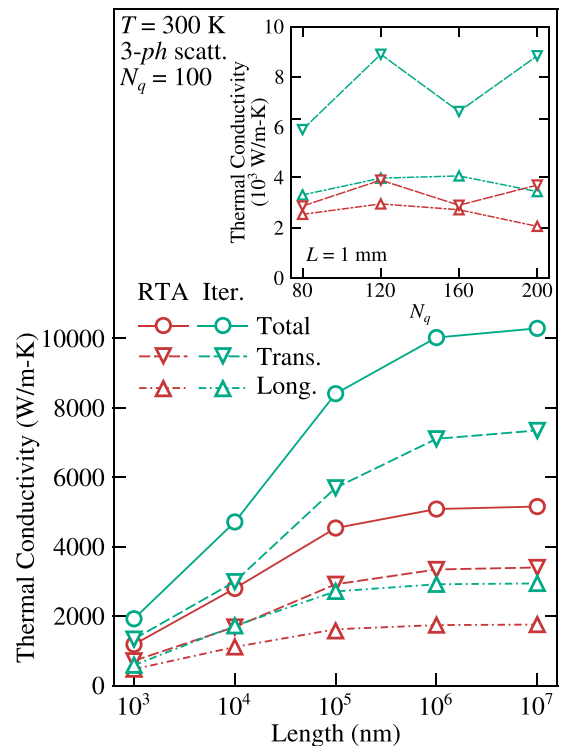

FIG. 2. The length-dependent thermal conductivity of SWCNT as obtained using the RTA (red) and iterative (cyan) solution of BTE by considering only three-phonon scattering. The results are obtained using a phonon wave vector grid of size $N_q = 100$. The variation of longitudinal and transverse modes thermal conductivity with a phonon wave vector grid is reported in the inset for a tube length of 1 mm. The contribution from transverse modes is not converged with the phonon wave vector grid for N_q up to 200.
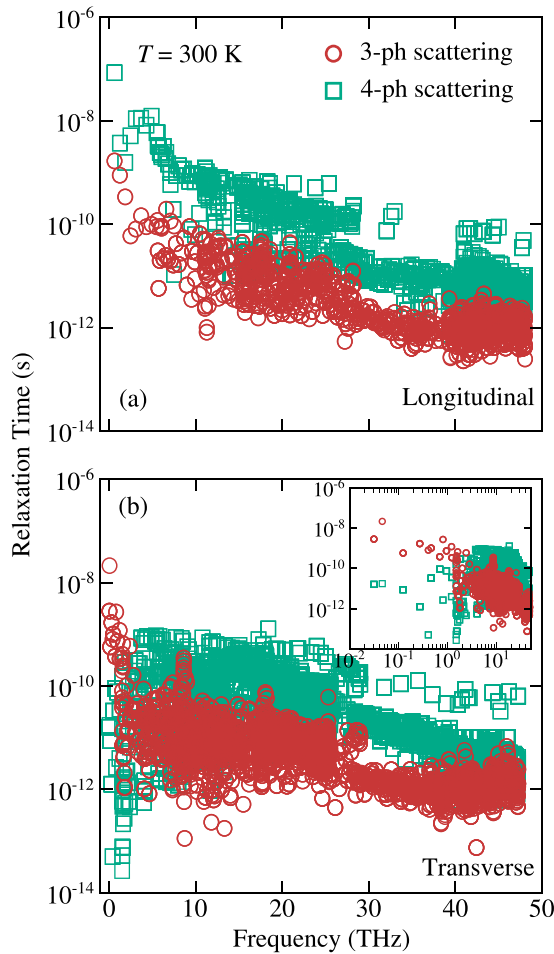
FIG. 3. The phonon relaxation times obtained by considering three-phonon (red) and four-phonon (cyan) scattering for (a) longitudinal and (b) transverse phonon modes. The low-frequency transverse phonon modes are unscattered via three-phonon processes but undergo scattering via four-phonon processes. The inset in (b) is the same as (b) on the log-frequency scale.
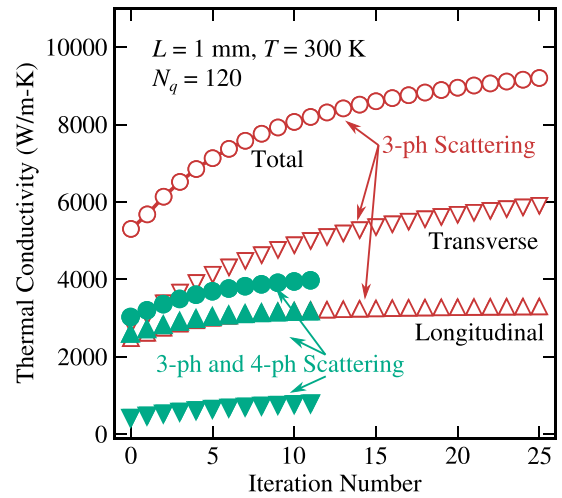

FIG. 4. The effect of four-phonon scattering on the thermal conductivity of SWCNTs. The thermal conductivities are obtained using the iterative solution of the BTE with iteration zero corresponding to the RTA solution of BTE. With the inclusion of four-phonon scattering, while longitudinal modes remain unaffected, the contribution of transverse modes decreases drastically. The contribution of transverse modes to the total thermal conductivity decreases from 64% to 25% with the inclusion of four-phonon scattering. With 3 ph and 4 ph scatterings, the iterative solution converges and the change in total thermal conductivity is within 1% between the last two iterations.

the κ obtained using DFT force constants converges to 5200 W/m-K using the RTA solution of the BTE (Fig. 2) and it compares well with the corresponding value of 6200 W/m-K reported by Lindsay *et al.* [7] using the Tersoff forcefield. Further, the κ obtained here using the iterative solution of the BTE is more than a factor of two higher than that obtained via the RTA solution. The mode-dependence of total κ in Fig. 2 shows that while the longitudinal modes contribution converges well with tube length, the transverse modes contribution is nonconverged and keeps increasing with tube length for tube lengths up to 1 mm. The inset of Fig. 2 further highlights this nonscattering of transverse modes via Umklapp three-phonon processes, where κ contributions from both longitudinal and transverse modes are converged with the phonon wave vector grid at the RTA level solution of the BTE (treating Normal processes also as resistive processes) but the contribution of transverse modes is not converged with the phonon wave vector grid with the iterative solution of the BTE even for grid sizes of 200. The effect of four-phonon scattering on the phonon relaxation lifetimes (not transport lifetimes)

is reported in Figs. 3(a) and 3(b) for longitudinal and transverse phonon modes. For longitudinal modes, the phonon scattering via four-phonon processes is weaker than that via three-phonon processes for all phonons. The same applies to transverse modes with frequencies larger than 2–3 THz. In contrast, when considering low-frequency transverse modes, the situation is reversed, with four-phonon processes significantly surpassing three-phonon processes in terms of phonon scattering strength by several orders of magnitude, i.e., the long wavelength phonon modes which are otherwise unscattered via three-phonon processes undergoing scattering with four-phonon processes. It is worth emphasizing that the relaxation times of several phonon modes are reduced to less than 10^{-12} s with the inclusion of four-phonon scattering. While several of these modes have $\omega_i \tau_i < 1$, which questions the quasi-particle-like description of phonons (as required by the BTE [30]), the contribution of these modes is less than 5% with only three-phonon scattering and reduces to 0% with four-phonon scattering (Fig. S2) [28].

The effect of four-phonon scattering on the predicted κ of SWCNTs using the iterative solution of the BTE is reported in Fig. 4. Iteration zero in Fig. 4 corresponds to the RTA solution of the BTE. As can be seen from the figure, the longitudinal modes contribution remains largely unaffected with the inclusion of four-phonon scattering. The contribution of transverse modes, however, reduces drastically: using the RTA solution of the BTE, the contribution of transverse mode reduces from more than 2800 W/m-K to less than 425 W/m-K with four-phonon scattering. This reduction in κ of transverse modes originates from Umklapp four-phonon processes, as even with

the iterative solution of the BTE, the contribution of transverse modes remains lower than 800 W/m-K (compared to around 6000 W/m-K with only three-phonon scattering).

It is worth mentioning that the phonon wave vector grid employed here for four-phonon scattering rate calculation is of size 120, which results in 14 400 phonon modes. This count is more than that reported recently for graphene by Han and Ruan [31], where authors found convergence of three- and four-phonon scattering limited κ for 9600 phonon modes but nonconvergence of three-phonon limited κ even with 345 600 phonon modes. Further, this study does not include the effect of temperature renormalization on interatomic force constants arising from atomic thermal displacements. As is shown recently for graphene [32], the thermal stochastic technique [33], which is the method of choice to capture this effect, is not applicable for materials with quadratic phonon dispersions.

V. CONCLUSIONS

In summary, the thermal conductivity of single wall carbon nanotube is evaluated numerically using the iterative solution of the Boltzmann transport equation by considering both three- and four-phonon scatterings with density functional theory-based harmonic, cubic, and quartic interatomic force constants see Supplemental Material [28]. The flexural and twisted phonon modes, which remain unscattered via Umklapp three-phonon processes, are found to undergo Umklapp scattering with four-phonon processes, resulting in a predicted thermal conductivity of 4000 W/m-K at 300 K.

The raw/processed data required to reproduce these findings is available on a reasonable request via email.

[1] J. Hone, M. Whitney, C. Piskoti, and A. Zettl, Thermal conductivity of single-walled carbon nanotubes, Phys. Rev. B **59**, R2514 (1999).

[2] P. Kim, L. Shi, A. Majumdar, and P. L. McEuen, Thermal transport measurements of individual multiwalled nanotubes, Phys. Rev. Lett. **87**, 215502 (2001).

[3] E. Pop, D. Mann, Q. Wang, K. Goodson, and H. Dai, Thermal conductance of an individual single-wall carbon nanotube above room temperature, Nano Lett. **6**, 96 (2006).

[4] J. Shiomi and S. Maruyama, Non-fourier heat conduction in a single-walled carbon nanotube: Classical molecular dynamics simulations, Phys. Rev. B **73**, 205420 (2006).

[5] D. Donadio and G. Galli, Thermal conductivity of isolated and interacting carbon nanotubes: Comparing results from molecular dynamics and the Boltzmann transport equation, Phys. Rev. Lett. **99**, 255502 (2007).

[6] C. W. Chang, D. Okawa, H. Garcia, A. Majumdar, and A. Zettl, Breakdown of Fourier's law in nanotube thermal conductors, Phys. Rev. Lett. **101**, 075903 (2008).

[7] L. Lindsay, D. A. Broido, and N. Mingo, Lattice thermal conductivity of single-walled carbon nanotubes: Beyond the relaxation time approximation and phonon-phonon scattering selection rules, Phys. Rev. B **80**, 125407 (2009).

[8] V. Lee, C.-H. Wu, Z.-X. Lou, W.-L. Lee, and C.-W. Chang, Divergent and ultrahigh thermal conductivity in millimeter-long nanotubes, Phys. Rev. Lett. **118**, 135901 (2017).

[9] D. Bruns, A. Nojeh, A. S. Phani, and J. Rottler, Heat transport in carbon nanotubes: Length dependence of phononic conductivity from the Boltzmann transport equation and molecular dynamics, Phys. Rev. B **101**, 195408 (2020).

[10] G. Barbalinardo, Z. Chen, H. Dong, Z. Fan, and D. Donadio, Ultrahigh convergent thermal conductivity of carbon nanotubes from comprehensive atomistic modeling, Phys. Rev. Lett. **127**, 025902 (2021).

[11] E. Fermi, P. Pasta, S. Ulam, and M. Tsingou, Studies of the nonlinear problems (1955), doi: 10.2172/4376203.

[12] J. Liu, T. Li, Y. Hu, and X. Zhang, Benchmark study of the length dependent thermal conductivity of individual suspended, pristine SWCNTs, Nanoscale **9**, 1496 (2017).

[13] Q.-Y. Li, K. Takahashi, and X. Zhang, Comment on "divergent and ultrahigh thermal conductivity in millimeter-long nanotubes", Phys. Rev. Lett. **119**, 179601 (2017).

[14] L. Lindsay, D. A. Broido, and N. Mingo, Diameter dependence of carbon nanotube thermal conductivity and extension to the graphene limit, Phys. Rev. B **82**, 161402(R) (2010).

[15] J. A. Thomas, R. M. Iutzi, and A. J. H. McGaughey, Thermal conductivity and phonon transport in empty and water-filled carbon nanotubes, Phys. Rev. B **81**, 045413 (2010).

[16] K. Sääskilahti, J. Oksanen, S. Volz, and J. Tulkki, Frequency-dependent phonon mean free path in carbon nanotubes from nonequilibrium molecular dynamics, Phys. Rev. B **91**, 115426 (2015).

[17] T. Feng and X. Ruan, Quantum mechanical prediction of four-phonon scattering rates and reduced thermal conductivity of solids, Phys. Rev. B **93**, 045202 (2016).

[18] T. Feng and X. Ruan, Four-phonon scattering reduces intrinsic thermal conductivity of graphene and the contributions from flexural phonons, Phys. Rev. B **97**, 045202 (2018).

[19] N. K. Ravichandran and D. Broido, Phonon-phonon interactions in strongly bonded solids: Selection rules and higher-order processes, Phys. Rev. X **10**, 021063 (2020).

[20] Y. Xia, K. Pal, J. He, V. Ozoliņš, and C. Wolverton, Particlelike phonon propagation dominates ultralow lattice thermal conductivity in crystalline Tl_3VSe_4, Phys. Rev. Lett. **124**, 065901 (2020).

[21] A. Jain, Multichannel thermal transport in crystalline Tl_3VSe_4., Phys. Rev. B **102**, 201201(R) (2020).

[22] A. Jain, Single-channel or multichannel thermal transport: Effect of higher-order anharmonic corrections on the predicted phonon thermal transport properties of semiconductors, Phys. Rev. B **106**, 045207 (2022).

[23] T. Yamamoto, S. Watanabe, and K. Watanabe, Universal features of quantized thermal conductance of carbon nanotubes, Phys. Rev. Lett. **92**, 075502 (2004).

[24] A. J. McGaughey, A. Jain, H.-Y. Kim, and B. Fu, Phonon properties and thermal conductivity from first principles, lattice dynamics, and the Boltzmann transport equation, J. Appl. Phys. **125**, 011101 (2019).

[25] S. Baroni, S. de Gironcoli, A. Dal Corso, and P. Giannozzi, Phonons and related crystal properties from density-functional perturbation theory, Rev. Mod. Phys. **73**, 515 (2001).

[26] P. Giannozzi, S. Baroni, N. Bonini, M. Calandra, R. Car, C. Cavazzoni, D. Ceresoli, G. L. Chiarotti, M. Cococcioni, I. Dabo, A. D. Corso, S. de Gironcoli, S. Fabris, G. Fratesi, R. Gebauer, U. Gerstmann, C. Gougoussis, A. Kokalj, M. Lazzeri, L. Martin-Samos *et al.*, QUANTUM ESPRESSO: a modular and open-source software project for quantum simulations of materials, J. Phys.: Condens. Matter **21**, 395502 (2009).

[27] J. P. Perdew, A. Ruzsinszky, G. I. Csonka, O. A. Vydrov, G. E. Scuseria, L. A. Constantin, X. Zhou, and K. Burke, Restoring the density-gradient expansion for exchange in solids and surfaces, Phys. Rev. Lett. **100**, 136406 (2008).

[28] See Supplemental Material at http://link.aps.org/supplemental/10.1103/PhysRevB.109.155413 for raw interatomic force constants and their dependence on calculation methodology and validity of quasi-particle description of phonons.

[29] D. Bruns, A. Nojeh, A. S. Phani, and J. Rottler, Nanotube heat conductors under tensile strain: Reducing the three-phonon scattering strength of acoustic phonons, Phys. Rev. B **104**, 075440 (2021).

[30] M. Simoncelli, N. Marzari, and F. Mauri, Unified theory of thermal transport in crystals and glasses, Nat. Phys. **15**, 809 (2019).

[31] Z. Han and X. Ruan, Thermal conductivity of monolayer graphene: Convergent and lower than diamond, Phys. Rev. B **108**, L121412 (2023).

[32] S. Alam, A. G. Gokhale, and A. Jain, Revisiting thermal transport in single-layer graphene: On the applicability of thermal snapshot interatomic force constant extraction methodology for layered materials, J. Appl. Phys. **133**, 215102 (2023).

[33] O. Hellman, P. Steneteg, I. A. Abrikosov, and S. I. Simak, Temperature dependent effective potential method for accurate free energy calculations of solids, Phys. Rev. B **87**, 104111 (2013).